ACS APPLIED MATERIALS & INTERFACES

Research Article

www.acsami.org

Catalytic Behavior of Lithium Nitrate in Li-O_2 Cells

Daniel Sharon,[†,⊥] Daniel Hirsberg,[†,⊥] Michal Afri,[†] Frederick Chesneau,[‡] Ronit Lavi,[†] Aryeh A. Frimer,[†] Yang-Kook Sun,[§] and Doron Aurbach*[,†]

[†]Department of Chemistry, Bar Ilan University, Ramat-Gan 52900, Israel

[‡]BASF SE, GCI/E - M311, Ludwigshafen 67056, Germany

[§]Department of Energy Engineering, Hanyang University, Seoul 133-791, South Korea

ABSTRACT: The development of a successful Li-O_2 battery depends to a large extent on the discovery of electrolyte solutions that remain chemically stable through the reduction and oxidation reactions that occur during cell operations. The influence of the electrolyte anions on the behavior of Li-O_2 cells was thought to be negligible. However, it has recently been suggested that specific anions can have a dramatic effect on the chemistry of a Li-O_2 cell. In the present paper, we describe how $LiNO_3$ in polyether solvents can improve both oxygen reduction (ORR) and oxygen evolution (OER) reactions. In particular, the nitrate anion can enhance the ORR by enabling a mechanism that involves solubilized species like superoxide radicals, which allows for the formation of submicronic Li_2O_2 particles. Such phenomena were also observed in Li-O_2 cells with high donor number solvents, such as dimethyl sulfoxide dimethylformamide (DMF) and dimethylacetamide (DMA). Nevertheless, their instability toward oxygen reduction, lithium metals, and high oxidation potentials renders them less suitable than polyether solvents. In turn, using catalysts like LiI to reduce the OER overpotential might enhance parasitic reactions. We show herein that $LiNO_3$ can serve as an electrolyte and useful redox mediator. NO_2^- ions are formed by the reduction of nitrate ions on the anode. Their oxidation forms NO_2, which readily oxidizes to Li_2O_2. The latter process moves the OER overpotentials down into a potential window suitable for polyether solvent-based cells. Advanced analytical tools, including in situ electrochemical quartz microbalance (EQCM) and ESR plus XPS, HR-SEM, and impedance spectroscopy, were used for the studies reported herein.

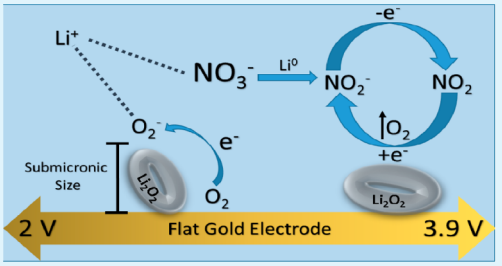

KEYWORDS: *Li-O_2 batteries, oxygen reduction reactions, oxygen evolution reactions, electrocatalysis, redox mediators, carbon cathodes*

INTRODUCTION

Extending the driving distance of electric cars is a strong incentive for the development of the next generation of batteries.[1,2] Technologies like lithium−sulfur and lithium−oxygen batteries could more than double the energy density of existing lithium ion batteries.[3] Indeed, over the past decade, increased efforts have been put toward the development of aprotic Li-O_2 cells. Early research gave seemingly optimistic results showing the great potential of this system. However, recently, progress has been impeded by difficulty in finding suitable cell components that will allow for prolonged cycling of Li-O_2 cells. Of the many challenges that need to be addressed in Li-O_2 cells, the stability of two components stand out: the carbon cathode[4] and the electrolyte solution.[5] These factors become prominent during both the oxygen reduction reaction (ORR) and the oxygen evolution reaction (OER). During ORR, the main damage occurs when the aprotic solvents react with reduced oxygen radicals, resulting in solvent consumption and side products that can clog the carbon cathode.[6−12] In addition, the cell's capacity is not fully exploited because ORR products like Li_2O_2 are nonconductive. This, in turn, limits the growth of the Li_2O_2 film formed by oxygen reduction to a few nanometers−allowing one to obtain only a low capacity that does not justify the great investment of money and time that has gone in to these problematic systems.[13] During the OER, both the cathode and the electrolyte solutions are damaged and decomposed. The carbon cathodes are corroded by the oxides, resulting in the formation of a nonconductive passivation layer composed of carbonate species that increase the overpotential. In addition, applying high potentials for the oxidation of the ORR products will also result in the oxidation of the electrolyte solution.[14]

Despite the many attempts to find solvents that are stable toward activated oxygen species, none were found to be fully resistant. Although these solvent were not completely stable, they did reveal features that can affect the ORR. One important solvent parameter is the Guttmann number;[15] thus, high donor number (DN) solvents like dimethyl sulfoxide (DMSO)[16,17] and dimethylacetamide (DMA)[18] are able to stabilize the soluble superoxide intermediate during ORR. Johnson et al.[19] suggested that, during the first reduction process, the formed LiO_2 is under equilibrium between two states. LiO_2 is either adsorbed on the electrode surface or dissolved in the electrolyte solution. In high DN solvents, the equilibrium favors the soluble LiO_2 moiety. The solubility enables the nonconductive Li_2O_2 to grow from the solution phase, leading to the formation

Received: May 13, 2015
Accepted: July 9, 2015
Published: July 9, 2015

DOI: 10.1021/acsami.5b04145
ACS Appl. Mater. Interfaces 2015, 7, 16590−16600

of larger particles. A similar effect was accomplished by adding water contamination to the electrolyte solution, which enhances the formation of soluble species.[20] Nevertheless, both solvent[21] and water[22] can also enhance parasitic reactions. Soluble charged species were also used for reducing the OER overpotential. Thus, redox mediators like LiI,[23] TMPO[24] and TTF[25] could oxidize Li_2O_2 by accepting charge at relatively low potentials and transfer it to the carbon cathode. However, caution is needed because recent work by Kwak et al.[26] showed that using LiI can also form additional side products.

The present paper reports our studies on the use of lithium nitrate ($LiNO_3$) as an electrolyte in polyether solutions that positively affects the ORR mechanism, reduces OER overpotential, and avoids the negative aspects mentioned above. $LiNO_3$ is also a well-known passivation agent for lithium metal.[27] Indeed, $LiNO_3$ is a key component in LiS batteries, where the shuttle mechanism of the polysulfide, occurring between the cathode and the lithium anode, can be mitigated by the passivation of the anode.[28,29] In Li-O_2 cells, $LiNO_3$ was first introduced as a passivation agent for Li metal in cells using amide solvents like DMA[18] because of the latter's high reactivity toward lithium metal.[30]

Cells containing $LiNO_3$ in amide solvents showed poor cycling performance because amide solvents tend to decompose in the presence of oxygen reduction.[31,32] However, one positive feature observed was the low OER overpotential obtained, which was associated with the redox behavior of $LiNO_3$ byproducts.[32] The use of $LiNO_3$ in other solvents also showed positive results. Thus, Kang et al.[33] report that $LiNO_3$ introduced into ether-based solvents decomposes on the carbon surface, forming nitrogen-containing groups that protect the carbon from corrosion at high oxidation potentials. Similarly, Sun et al.[34] added $LiNO_3$ to DMSO to protect the lithium anode from reacting with DMSO. They also observed a lower average potential for the OER.

Recent work by Gunasekrar et al.[35] suggested that anions that can complex with lithium cations can reduce the lithium Lewis acidity, thereby temporarily preventing its tendency to bind to reduced oxygen moieties. As a result, soluble species like superoxide can take part in the growth mechanism. This phenomenon is based on the strength of the ionic association of the electrolyte in the aprotic solvent. Lithium nitrate, while being highly soluble in ether solvents, can be considered a highly associated salt in polar aprotic solvent. This was demonstrated by studying the FTIR, Raman, and differential scanning calorimetry (DSC) of various lithium electrolytes.[36−39] As a result, nitrate anions can coordinate strongly to the solvated lithium cation, leading to slower interactions between moieties formed by oxygen reduction like superoxide and Li ions.

Screening studies on the stability of major aprotic solvents for Li-O_2 cells has led us to conclude that the polyether family is sufficiently stable on both the anode and cathode interfaces to enable fundamental studies, as presented herein.[40] Therefore, carried out in diglyme, we compare two salts: the standard 1 M LiTFSI and 1 M $LiNO_3$. Although solvent stability remains a key issue, we demonstrate that using $LiNO_3$ electrolyte in polyether solutions can contribute significantly to a better performance of Li-O_2 cells.

RESULTS

The voltage profiles of ORR and OER in 1 M $LiNO_3$ and LiTFSI solutions in diglyme with monolithic carbon paper cathodes are presented in Figure 1a. The discharge process in the LiTFSI solution occurs at a slightly higher overpotential

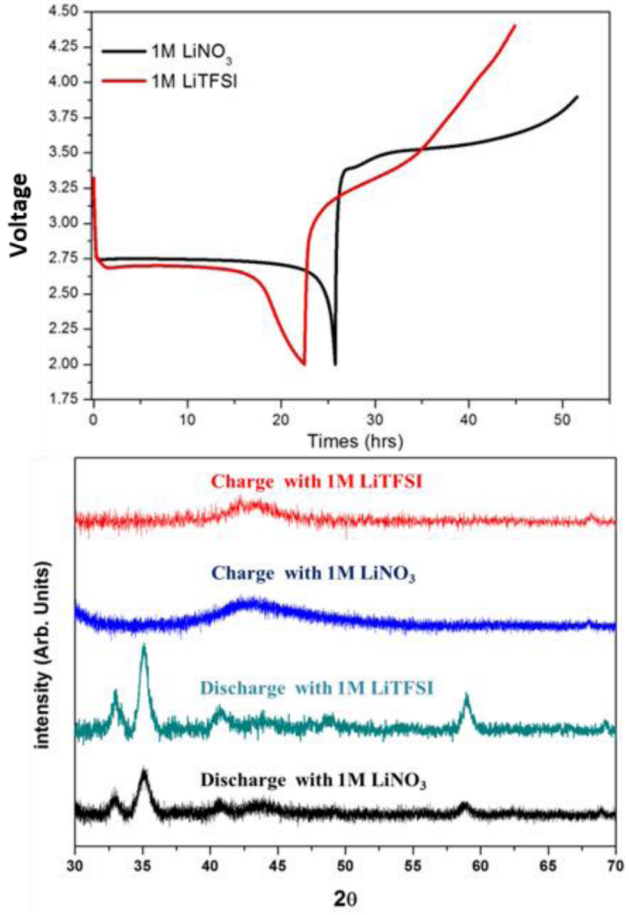

Figure 1. (a) Voltage profiles of carbon paper electrodes in diglyme 1 M LiTFSI (red curve) and diglyme 1 M $LiNO_3$ (black curve) solutions upon ORR and OER at a current density of 0.1 mA cm^{-2} and (b) XRD patterns of cathodes cycled in diglyme 1 M LiTFSI and 1 M $LiNO_3$, as indicated.

than that relevant to the $LiNO_3$ solution. A more prolonged ORR can take place in $LiNO_3$ solutions, and the voltage drops sharply when the process ends. (This drop is due to blockage of the electrodes by deposition of the ORR products.) In the LiTFSI solution, the voltage drops at a moderate rate, suggesting a different ORR mechanism.

Figure 1b shows the XRD patterns of cycled carbon electrodes (after ORR and OER, as indicated) in both 1 M $LiNO_3$ and LiTFSI solutions in diglyme under oxygen atmosphere. After being discharged to 2 V, the spectra related to both electrolyte solutions exhibit peaks characteristic of crystalline Li_2O_2. It is important to note that the XRD patterns of these carbon cloth electrodes cannot provide reliable quantitative analysis but do help in the identification of the main products formed. The pattern for the cathodes charged to 4.45 V in 1 M LiTFSI solution shows that all of the peroxide was removed during the OER. Interestingly, the same pattern was obtained in 1 M $LiNO_3$ solution but with a cutoff voltage of only 3.9 V.

The OER in the LiTFSI solution containing cells begins at lower overpotentials around 3.00−3.4 V; however, as we proceed, the voltage increases up to 4.45 V as full reversible

DOI: 10.1021/acsami.5b04145
ACS Appl. Mater. Interfaces 2015, 7, 16590−16600

cycles are attained. The voltage of the $LiNO_3$-containing cells jumps suddenly to around 3.50 V but remains relatively stable during the entire OER, reaching 3.9 V at the end of the charging process. The differences between the LiTFSI- and $LiNO_3$-containing cells in the early oxidation process can be explained by the morphological difference of the deposits obtained by ORR in these solutions. Ganpathy and co-workers[41] observed two main oxidation processes during OER. At low potentials, the amorphous Li_2O_2 is decomposed. As the potential is raised, the crystalline Li_2O_2 is oxidized starting with the smaller crystals. Our HR-SEM images support this assumption with the particles formed on the cathodes of the 1 M $LiNO_3$ solution-containing cells observed to be much larger than those formed on the cathodes in LiTFSI solution-containing cells. The oxidation process starts around 3 V in the LiTFSI solution, indicating that most of the ORR products are small crystals or amorphous deposits of Li_2O_2.

However, the most important phenomena observed in the $LiNO_3$ solutions is the relatively low voltage (~4 V) required to complete the OER. This feature is essential for cells based on polyether solvents, which undergo oxidation at potentials of around 4 V, which further intensifies as the potential increases to 4.5 V. In addition to this solvent oxidation in Li-O_2 cells containing ethereal solutions, the carbon cathode corrodes by reacting with the peroxides at these high potentials. Both of these side reactions can result in blockage of the cathode matrices during several ORR-OER cycles only.[14]

The cycling behavior of the cells containing 1 M $LiNO_3$ or LiTFSI solutions is presented in Figure 2. The cell capacity in both cases was limited due to capacity fading occurring when we attempted to fully discharge the cells. Nevertheless, the changes occurring during cycling are visible even in these short discharge processes. In the first charging process of the $LiNO_3$-containing cells, the oxidation voltage reaches 3.9 V. The similarity between the oxidation potentials of the cell without limitation (Figure 1a) and the partially discharged cells (Figure 2) are by no means trivial, as we expect higher OER overpotentials for the cells discharged to 2 V. The consistency in the values should result from the thickness of the ORR product layers formed on the carbon cathodes. The long discharge process should form more nonconductive products like Li_2O_2 on the cathode surface, which would lead to high overpotentials. The lack of potential change implies that the OER process involves a mobile charged species that can transfer charge from the nonconductive layer to the cathode. In such a scenario, the thickness of the layer does not really affect the overpotential. The increase in the OER overpotential during cycling can be related to irreversible reactions like electrolyte and solvent decomposition that lead to carbon clogging and consumption of solution components.

Conversely, the potential during the first charge of the cells containing LiTFSI is different when we only partially discharge them. The cells with the limited capacity reached 4.1 V during a first charge compared to 4.45 V for cells discharged to 2 V, as shown in Figure 1a. This change supports an OER mechanism that is affected by the quantity of the products formed during the ORR. However, even when the cells' capacity is limited, upon repeated cycling with LiTFSI solutions, the voltage increases and stabilizes at 4.45 V.

HR-SEM images of discharged cathodes are presented in Figure 3. Cathodes polarized to 2 V in 1 M LiTFSI are coated by networks of nanosize wires (Figure 3b) along with bigger aggregates constructed from these nanosize wires. The

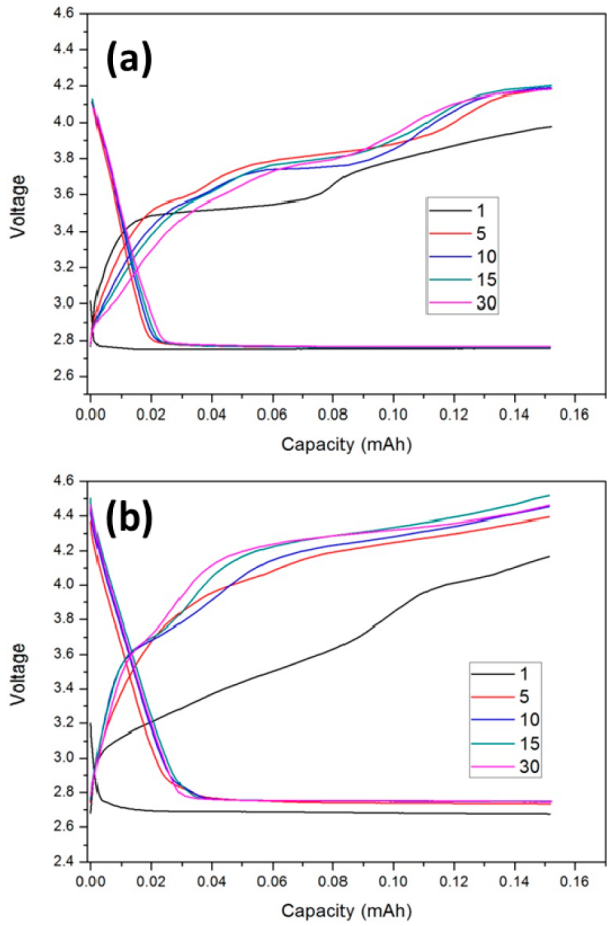

Figure 2. Cycling behavior of a Li-O_2 cells with (a) 1 M $LiNO_3$ or (b) 1 M LiTFSI solutions in diglyme at a current density of 0.1 mA cm^{-2} using carbon paper cathodes.

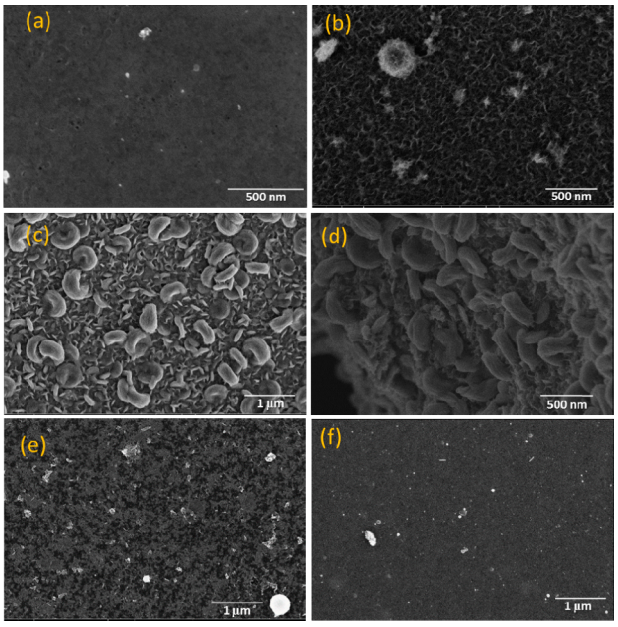

Figure 3. HR-SEM of carbon paper electrodes: (a) pristine electrode, (b) electrode polarized to 2 V in 1 M LiTFSI solution, (c and d) electrode polarized to 2 V in $LiNO_3$ solution, (e) electrodes polarized after ORR to 3.9 V in 1 M $LiNO_3$ solution, and (f) electrode polarized after ORR to 4.5 V in 1 M LiTFSI solution.

DOI: 10.1021/acsami.5b04145
ACS Appl. Mater. Interfaces 2015, 7, 16590−16600

discharged cathode surface in 1 M $LiNO_3$ solution is covered by large toroid-shaped particles in the submicron range. Between these big structures there are smaller sized, arch-shaped particles.

We surmise that, in both cells, the nucleation process starts with small wire-shaped fragments that eventually grow to be toroidal. In the cells containing LiTFSI solution, the grains stop growing and do not collide with other nuclei, resulting in a homogeneous distribution of nanosized particles that cover the carbon surface. The submicronic products in the $LiNO_3$-containing cells were not limited, as observed in the LiTFSI-containing cells.

On the basis of the literature, it can be assumed that the main product formed during ORR in Li-O_2 cell is Li_2O_2, which is insoluble and has a very low conductivity. This in theory should lead to a bottom up growth that stops at the nanometeric layer due to its inability to transfer charge to the outside (solution side) of the deposited Li_2O_2 layer. This should be the situation in LiTFSI solutions. The appearance of large particles in $LiNO_3$ solutions must involve soluble and charged moieties in solution, which assist a top down growth mechanism. In such growth, charged species can diffuse in the solution and transfer charge in all dimensions of the particles, leading to larger products.

Figure 3f shows an SEM picture of an electrode charged up to 4.5 V in 1 M LiTFSI diglyme solution. As expected, during charging, the small Li_2O_2 particles are oxidized, and the carbon cathode returns to its initial state. This assumption that this behavior is reversible is inaccurate. Although Li_2O_2 is oxidized in these potentials, as can be seen from the XRD patterns of the cathodes after OER, there is much evidence that charging carbon cathodes to more than 4 V results in solvent oxidation and worse, to carbon corrosion that leads to cell failure. Irreversible processes may occur on charged cathodes in 1 M $LiNO_3$ solutions as well, as shown in Figure 3e; although the big Li_2O_2 particles formed by ORR are absent, the carbon fibers are still covered with a rough surface after undergoing OER. Evidently avoiding high oxidation potentials does not guarantee that the carbon surface will not be damaged.

The impedance spectroscopy of the cathodes in 1 M LiTFSI and 1 M $LiNO_3$ solutions at different states of charge are presented in Figure 4a and b, respectively. The impedance measured at OCV is higher in the $LiNO_3$ solution. During discharge, the impedance of both cells increases. This can be attributed to the formation of a layer of nonconductive products on the carbon surface;[13] nevertheless, the impedance of the electrode treated in the $LiNO_3$ solution is much higher after the first discharge. This "insulator" behavior matches what we see in the SEM images after ORR (Figure 3c), a thick submicronic layer of products covering the carbon electrodes and blocking the pores. In turn, the thin nanosized layer growing on the cathode during ORR in the LiTFSI solution (Figure 3b) may allow more surface conductivity. This means that, even after full discharge to 2 V, the carbon surface is not fully blocked.

At the end of the charge process, which occurs at 3.9 V in the $LiNO_3$ and at 4.5 V in the LiTFSI solutions, different impedance spectra are observed. For cells with the LiTFSI solution, the cathodes' impedance increases after charging even though most of the ORR products are oxidized, and this should result in a decrease of the impedance. Nevertheless, because we reach high oxidation potentials, we also corrode the carbon[14] and oxidize the solvent, which in turn leads to the passivation of the cathode and an increase in its impedance. It can be said that

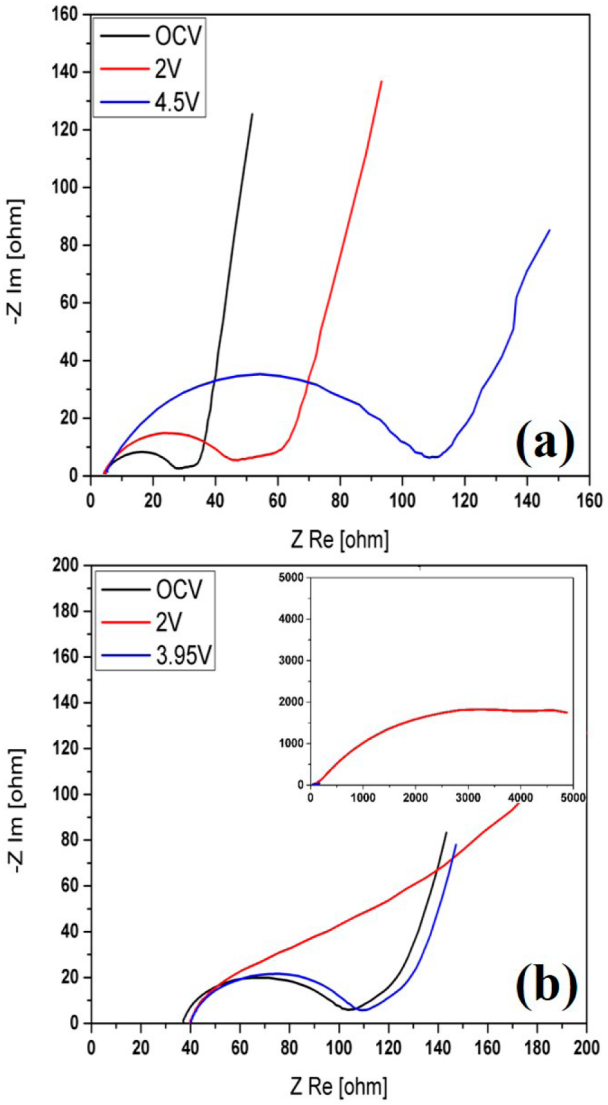

Figure 4. Impedance spectra (Nyquist plots) measured from carbon paper cathodes during the first cycle of Li-O_2 cells with diglyme solutions of (a) 1 M LiTFSI and (b) 1 M $LiNO_3$. The voltages in which the measurements were carried out are indicated therein.

the formation of new passivation layers during oxidation overcomes the removal of the ORR product layer. In contrast, the impedance of the cathodes in cells containing $LiNO_3$ solution decreases at the end of the charge process. In this latter scenario, the removal of the thick product layer prevents the formation of a new oxidation layer, and thus, the impedance decreases, returning to values similar to those measured initially at OCV.

The mechanism of ORR and OER in $LiNO_3$ solutions is connected to their intrinsic instability in Li-O_2 cells. As was recently discussed,[42] NO_3^- ions are reduced in ethereal solutions at potentials below 1.8 V relative to that of Li. Hence, NO_3^- anions can be easily reduced by the Li metal anodes to NO_2^- anions. Figure 5 shows UV−vis spectra of $LiNO_3$ solutions, both fresh and those aged in contact with Li metal. The spectrum of the latter shows the typical nitrite peak at 350 nm.[42−44] The inevitable presence of NO_2^- moieties in these cells dramatically affects the OER in $LiNO_3$ solutions, as discussed later.

DOI: 10.1021/acsami.5b04145
ACS Appl. Mater. Interfaces 2015, 7, 16590−16600

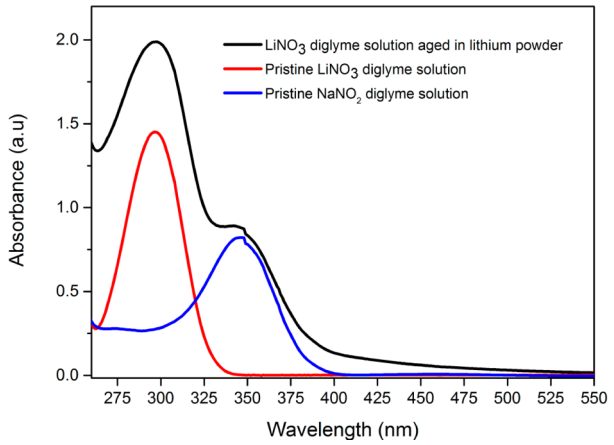

Figure 5. UV−vis spectra of pristine diglyme $LiNO_3$ solution (red curve), diglyme $LiNO_3$ solution stored 48 h with lithium metal powder (black curve), and pristine diglyme $NaNO_2$ solution in argon atmosphere (blue curve).

To examine the impact of 1 M $LiNO_3$ diglyme solutions on the surfaces of carbon cathodes, XPS analysis was carried out. The general elemental composition of the surface films obtained from XPS measurements was calculated. The pristine electrode contains 95% carbon and 5% oxygen. By discharging the cell to 2 V, a carbon cathode that is covered by 33% oxygen and 21% Li is obtained, supporting the formation of a lithium- and oxygen-rich species on the surface. The small amount (1.05%) of nitrogen found on the carbon surface is associated with the electrolyte decomposition. Upon charging to 3.9 V, most of the oxygen was removed from the surface, leaving only 8% oxygen. The increase in oxygen content as compared to the pristine state (5% oxygen) is presumably related to the oxidation of the carbon surface or to deposits resulting from irreversible side reactions. The nitrogen content on the cathode slightly increases to 1.37% after the end of the OER. The presence of nitrogen on the cathodes after both ORR and OER proves the irreversible nature of the reactions that form these species on the electrodes.

Figure 6 shows the high-resolution XPS C 1s and N 1s spectra of cycled carbon cathodes.

The discharged cathode C 1s spectrum contains two high binding energy peaks in addition to the carbon paper peak at 284.4 eV, namely, the carbonate peak at 289.8 eV and a peak at 286.0 eV that could correspond to a methyl carbonate group. In addition, a shoulder between 286.5 can be correlated to different carbonyl or alkoxy carbons. The absence of carbonate peaks in the XRD pattern and the low concentration of Li_2O_2 on the carbon surface both suggest that some of the decomposition products are surface phenomena that deposit on the bulk Li_2O_2 during the discharge process. The low potentials applied during discharge support the assumption that this Li_2CO_3 is related to solvent decomposition and not to the reaction between the peroxide and the carbon electrode.

The N 1s spectrum of the discharged cathode reveals the presence of a variety of nitrogen-based groups. At high binding energies, we observe the 408.4 and 404.8 eV peaks that may correspond to the NO_3^- and NO_2^- groups, respectively. The observation of solvated lithium nitrate on the cathode surface has been observed in previous studies.[33] The strong ionic association ability of $LiNO_3$ in diglyme can help to crystallize the salt and deposit it on the cathode surface.[36,37] At lower

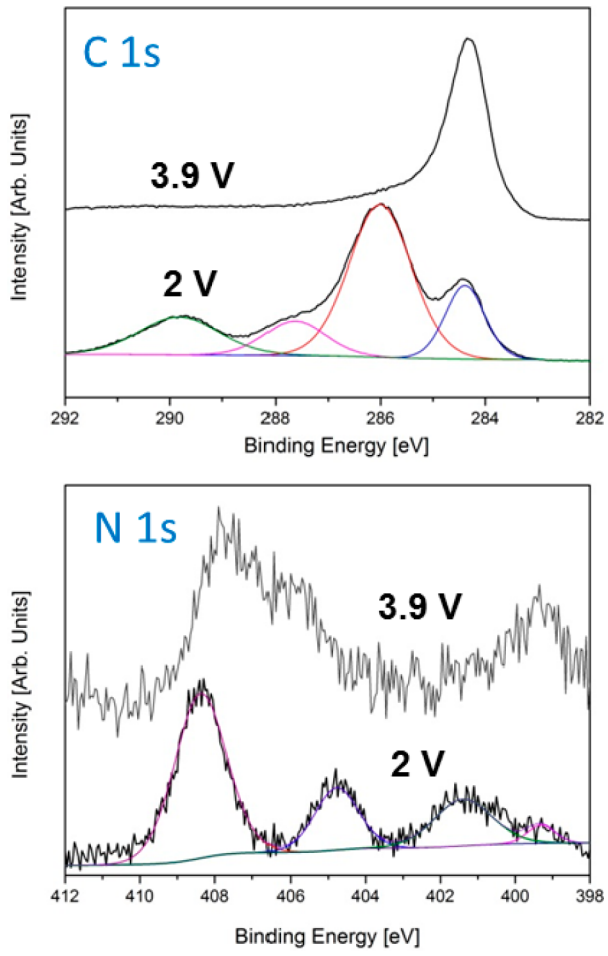

Figure 6. C 1s and N 1s XPS spectra of cycled carbon cathodes taken from Li-O_2 cells containing 1 M $LiNO_3$ diglyme solution discharged to 2 V and then discharged and charged to 3.9 V.

binding energies, a broad peak at 401.4 and a shoulder at 399.4 eV are observed, associated with amine groups, nitrogen-based heterocyclic compounds, and lithium hyponitrite at lower binding energies. The origin of these nitrogen groups is likely to be the reduction of the electrolyte on the Li anode. In previous work, we identified similar compounds on lithium metal electrodes that were aged in ethereal solutions containing $LiNO_3$.[27] Hence, the appearance of N−C, N−O, and N−H peaks can be associated with reactions between the ether solvent, the nitrate, and reduced oxygen. Kang et al. suggested that $LiNO_3$ can react with oxygenated groups located on the carbon cathode, leading to C−N bonds on the surface.[33] To avoid reactions between the carbon and the electrolyte, we reduced the carbon in Ar/H_2 to limit the presence of any C−O bonds. Nevertheless, the presence of C−N and N−H on the lithium anode proves that surface groups on the carbon cathodes are not necessarily essential for these surface reactions. A possible scenario may involve decomposition of the diglyme by LiO_2 or Li_2O_2. These fragments can then interact with NO_3^- or NO_2^- to form C−N, C−O, and N−H species on the cathode surface.

The C 1s spectrum of the cathode after charging confirms that Li_2O_2, Li_2CO_3, Li alkoxy, and Li alkyl carbonate species, if formed in the course of the ORR, are oxidized at voltages below 3.9 V. The ability to remove Li_2CO_3 below 3.9 V is very impressive because the potentials reported for the oxidation of

DOI: 10.1021/acsami.5b04145
ACS Appl. Mater. Interfaces 2015, 7, 16590−16600

carbonates are relatively high, beyond 4 V.[45] However, the N 1s spectrum of the charged cathode exhibits irreversible behavior with respect to the nitrogen moieties. The surface characterization of cycled cathodes indicates that polyether-based electrolyte solutions are unstable toward ORR, as was previously reported.[10,46,47] The $LiNO_3$ decomposition and crystallization on the cathode might well cause blockage of the carbon surface. Although diglyme decomposition products, like carbonates and alkoxide species, are oxidized during OER, these side reactions leave their mark on the cell's performance. The increase in the overpotentials and capacity fading during prolonged cycling are unavoidable with current electrolyte solutions.

To follow the transformations taking place during cell operations, we used electrochemical quartz crystal microbalance (EQCM)-containing platinum working electrodes (deposited on thin quartz crystals) that simultaneously measure the voltammetric and gravimetric response. Figure 7 shows the EQCM response of these Pt on quartz electrodes in cells containing $LiNO_3$ (black) and LiTFSI (red) solutions in diglyme.

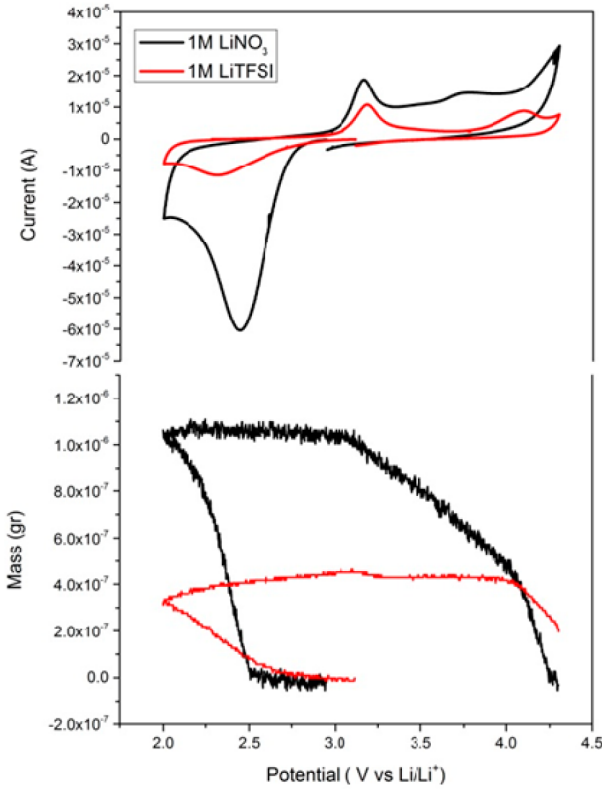

Figure 7. Cyclic voltammetry (scan rate of 5 mV/s) and EQCM response of platinum disks deposited on thin quartz crystals in diglyme 1 M $LiNO_3$ (black) and 1 M LiTFSI (red) solutions.

Under oxygen atmosphere, we observe the expected ORR peak during the cathodic scan. Reversing the scan to an anodic one, we see one peak between 3 and 3.5 V and another oxidation process above 4 V. The mass response of the QCM is correlated well with the ORR: as the cell starts the reduction process, we observe mass accumulation on the crystal. From m.p.e. calculations, we obtained that, for a one electron transfer, we accumulate a mass of 25 ± 2 g, depending on which range of ORR voltages we choose to focus. These values can be attributed to lithium oxygen species like Li_2O_2 (45.88 g/mol) if the reaction taking place is a direct two electron transfer of 22.9 g per electron.[10]

Sweeping to the anodic scan, we observe two slopes associated with mass removal. The first process is accompanied by only a slight decrease of mass and occurs during the first oxidation peaks between 3.0 and 3.5 V. At higher potentials (>4 V), we observe an oxidation peak and a considerable amount of mass removal from the cathode. However, it does not return to the initial conditions, suggesting that not all of the ORR products were removed during oxidation. The second mass removal process above 4 V can be affected by the oxidation of the polyether solvent. Interestingly, it was recently reported that Li_2O_2 in LiTFSI solutions is oxidized at the same potential as polyether solvents.[48,49] The researchers posited that formation of charged fragments by the decomposition of the solvent during OER can help to oxidize the nonconductive Li_2O_2 in much the same way as redox mediators.[48]

The voltammetric and gravimetric responses of these EQCM experiments in $LiNO_3$ solutions are much more pronounced than in LiTFSI solutions. The plots in Figure 7 clearly indicate that the ORR and OER are more intensive in the former solutions. Because of the better resolution obtained in the QCM data related to $LiNO_3$ solutions, we can distinguish between three different processes transpiring during ORR. From 2.8 to 2.5 V, more than 25% of the charge was transferred; however, no mass accumulates. The absence of gravimetric response implies that soluble species were formed at the start of the ORR. From 2.5 to 2.3 V, we observe a slope that corresponds to an m.p.e. of 31 g. This value is associated with the absorbance of reduced oxygen on the platinum surface. The last process is located between 2.3 and 2.0 V, and the mass response exhibits a small slope with an average value of 25.3 ± 2 g per electron transfer. This is linked to the formation of Li_2O_2, which accumulates on the electrode as the main product of the overall ORR, as is obvious from the XRD measurements

During OER in the $LiNO_3$ solution, the accumulated mass is removed from the electrode on the quartz crystal in two defined slopes. The first oxidation process starts around 3.2 V and continues up to 4 V. During the mass removal, we can also observe an additional peak between 3.6 and 3.9 V, which is discussed later. The next slope (>4 V) is similar to that observed in the LiTFSI solution and can be associated with the oxidation of the polyether solvent. However, unlike the LiTFSI solution, a significant amount of mass is removed before 4 V, pointing to a catalytic effect of the nitrate-related moieties.

The cyclic voltammetric response of Pt electrodes (using the EQCM cell) in 1 M $LiNO_3$ diglyme solution in argon atmosphere, shown in Figure 8a, helps us to understand the catalytic behavior of $LiNO_3$. Extremely important is the irreversible anodic process, expressed as a peak around 3.6 V. This process is intensified in the presence of oxygen. Figure 8b shows the voltammetric response at several scanning rates of a Pt electrode in LiTFSI/diglyme solution containing $NaNO_2$. It clearly shows an anodic peak at around 3.6 V with a corresponding cathodic peak around 3.4−3.5 V associated with the oxidation of NO_2^- to NO_2.

The cathodic process seen in Figure 8b is absent when the potentials are scanned anodically too far beyond the 3.6 V peak (e.g., to potentials higher than 4 V) as shown in Figure 8a. This is probably due to follow up oxidation of the NO_2 that is formed. The nitrite ions present in Li-O_2 cells containing $LiNO_3$ solutions, as demonstrated above, catalytically affect the

DOI: 10.1021/acsami.5b04145
ACS Appl. Mater. Interfaces 2015, 7, 16590−16600

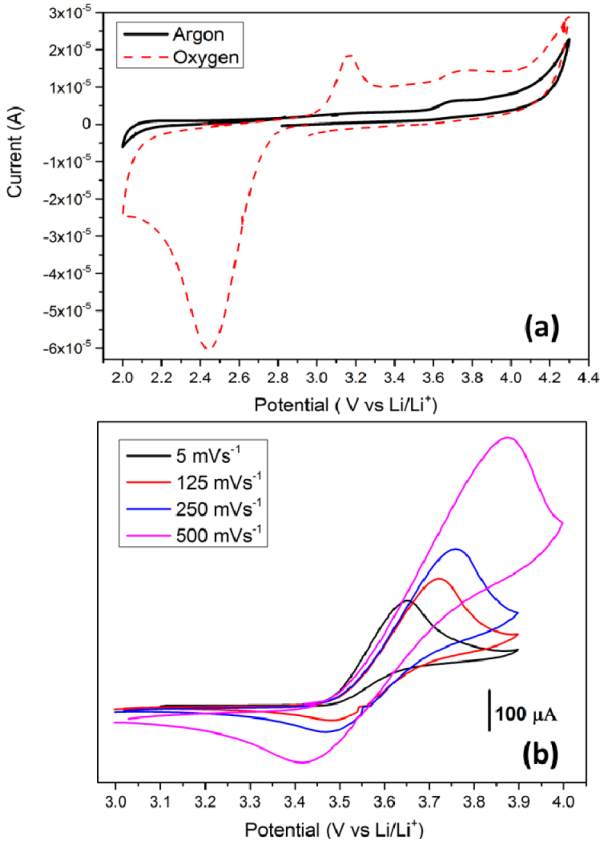

Figure 8. Cyclic voltammograms of Pt electrodes in (a) 1 M $LiNO_3$ diglyme solution under oxygen and argon atmospheres with a scan rate of 5 mV/s and in (b) a 0.2 M LiTFSI and 0.02 M $NaNO_2$ diglyme solution under argon atmosphere with different scan rates.

OER in $LiNO_3$ solutions. Because of their negative charge, nitrate and nitrite anions cannot oxidize Li_2O_2 by themselves, as is indeed evident by its accumulation on the cathode surface upon ORR in these solutions. We suggest that only NO_2, formed by oxidation of NO_2^- around 3.6−3.8 V, can function as a redox mediator in the solution phase that oxidizes the Li_2O_2 precipitants at potentials below 4 V. The ability of the soluble NO_2 to react with species on the carbon surface enables the oxidation of thick Li_2O_2 layers formed by the ORR at relatively low overpotentials. Even trace NO_2^- moieties in solution are enough to form active NO_2 below 3.8 V that can oxidize all the Li_2O_2 precipitated during ORR below 4 V via a shuttle interaction of the NO_2/NO_2^- couple.

The difference between $LiNO_3$ and LiTFSI solutions during ORR is well demonstrated in both the voltammetric and gravimetric responses of the EQCM measurements. As mentioned above, the association/dissociation behavior of the lithium salt in ether solvents can explain the differences. With dissociated salts like LiTFSI, the Li cations in solution are surrounded by solvation shells and are fully separated from the anions. By contrast, NO_3^- anions remain associated with the Li cations although they are surrounded by a solvation shell.[36,37,50] This latter phenomenon can indirectly affect the ORR mechanism. In recent work, Gunasekara et al.[35] report that associated salt anions that coordinate with the lithium cation reduce the Lewis acidity of the Li^+ ions. This in turn makes them less reactive toward superoxide radical anions that may well be formed by reduction of molecular oxygen in nonaqueous solutions. As a result, cell performance parameters like capacity and overpotential are affected. In the $LiNO_3$ ethereal solutions, the oxygen atoms of the nitrate anions are strongly associated with the Li^+ ions.[36] Consequently, the interaction of the oxygen radical anions, formed by oxygen reduction (superoxide and peroxide moieties[41]), with Li ions are not immediate, and rapid precipitation may be retarded. This in turn affects the process of molecular oxygen reduction, as is indeed observed in the EQCM response, which verifies the formation of mobile oxygen species. We hoped to be able to trace superoxide and peroxide moieties in $LiNO_3$ diglyme solutions formed by oxygen reduction using Raman and EPR measurements (see experimental description in ref 26). Several in situ ESR measurements during ORR in both solutions were carried out in the framework of the present studies, but they were not conclusive. The analysis of these measurements is difficult, and work is still in progress.

Another consequence of the presence of soluble charged species during ORR is a change in the crystal growth mechanism. In experiments that contained contaminations of water as a source of soluble charge species, submicronic toroidal-shaped Li_2O_2 were observed on the cathode surface of Li-O_2 cells.[22,51] Similarly, in our cells, the oxygen reduction products gain meta-stability due to the interactions of nitrate anions with Li cations in solution. When they reach a certain concentration near the electrode surface, they undergo inevitable interactions with the Li ions and precipitate as Li peroxide. In this way, the nonconductive Li_2O_2 particles thus formed can reach submicron ranges, as clearly presented in the SEM images of Figure 3.

To better focus on the effect of $LiNO_3$ on ORR in the ethereal solutions, we replaced the carbon cathodes with flat gold electrodes with negligible surface area. The discharge profiles of the gold cathodes in $LiNO_3$ and LiTFSI diglyme solutions are shown in Figure 9a. In both solutions, the voltage profiles of the gold electrodes somewhat resemble those obtained with the high surface area carbon cathodes during ORR and OER (Figure 1a). The low OER overpotential obtained in the $LiNO_3$ solution is not related to the nature of the electrodes but rather clearly reflects the catalytic effect of the NO_2/NO_2^- redox couple, as described above.

In terms of overpotential values, we do not see big differences between gold and activated carbon electrodes. However, in terms of capacity values, with gold electrodes, the ORR capacity in $LiNO_3$ solutions is by far higher than that obtained in LiTFSI solutions. Because gold electrodes possess low surface area, we expect a fast termination of the discharge process (occurring via a bottom−up precipitation mechanism) as less specific surface is available to contain deposits of Li_2O_2. Indeed, in LiTFSI solutions, the ORR voltage profile reaches 2 V very quickly, as can be seen in Figure 9a. This reflects little accumulation of Li_2O_2 on the gold surface until the electrode is fully blocked. The SEM image of a gold electrode discharged to 2 V in 1 M LiTFSI solution is presented in Figure 9c. The thin layer deposit on the gold surface correlates well to the short discharge process seen in the voltage profile. However, as we observed with carbon cathodes, a thick layer of Li_2O_2 particles is formed in $LiNO_3$ solutions on the gold electrodes during their polarization to 2 V under oxygen atmosphere; this is evident from the SEM image in Figure 9b and correlates well to the wide plateau in Figure 9a.

Thus, using gold cathodes with low surface area helps to elucidate how the nature of the anion can affect the ORR/OER mechanisms in polyether solutions. When using high surface

DOI: 10.1021/acsami.5b04145
ACS Appl. Mater. Interfaces 2015, 7, 16590−16600

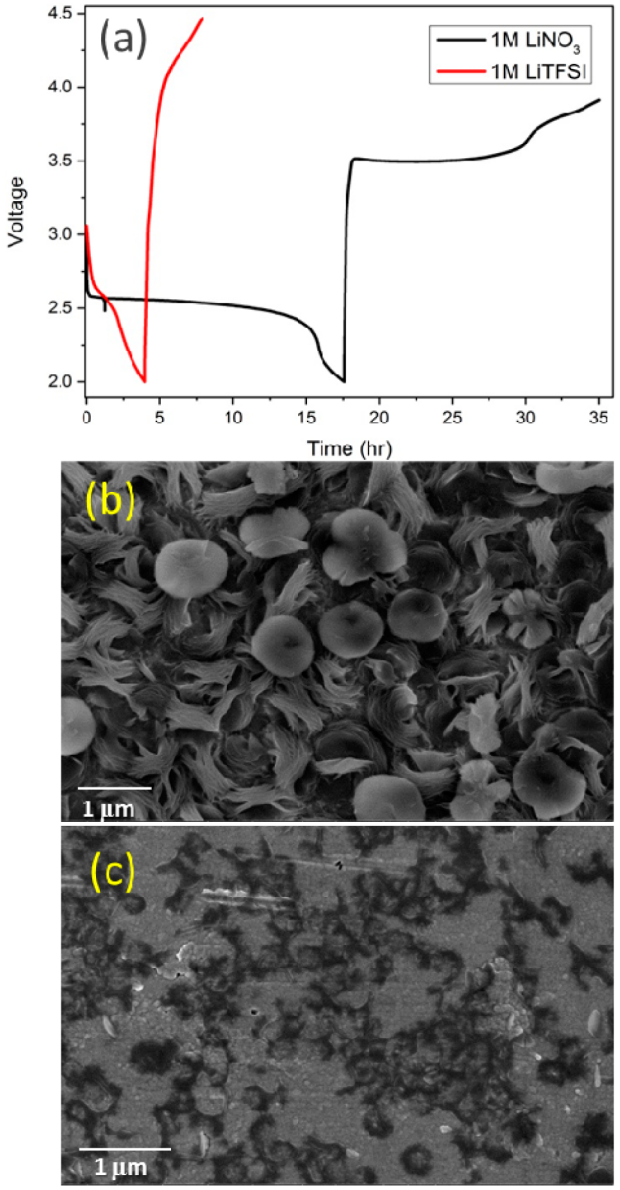

Figure 9. (a) Voltage profiles of gold electrodes in diglyme 1 M LiTFSI and diglyme 1 M $LiNO_3$ solutions upon ORR and OER; (b) HR-SEM images of gold electrodes discharged to 2 V in $LiNO_3$ diglyme solutions; (c) Same as (b) in LiTFSI diglyme solutions.

area carbon cathodes, their cathodic polarization in $LiNO_3$ solutions under oxygen atmosphere promotes ORR, yielding larger product yields than those obtained in LiTFSI solutions. However, we see only a small difference between these Li salt solutions in the measured ORR discharge capacity despite the advantage of the $LiNO_3$ electrolyte in promoting the ORR, as discussed above. When using LiTFSI electrolyte, the relatively simple bottom up mechanism of Li_2O_2 precipitation forms nanometric Li_2O_2 particles that can fit well into the pores of the carbon cathode and homogeneously cover the entire carbon surface. By contrast, when NO_3^- serves as the anions, we form submicronic Li_2O_2 particles that can clog the carbon pores and, therefore, reduce the free sites for Li_2O_2 nucleation and growth.[52] Considering all of these factors together, it is not surprising that ORR on activated carbon electrodes in $LiNO_3$ solutions demonstrates only a slightly higher capacity than in LiTFSI solutions. However, when flat cathodes like gold surfaces are employed, the top-down Li_2O_2 precipitation mechanism in $LiNO_3$ solutions (as explained above) enables the growth of a thick ORR product layer, thus promoting a long-term oxygen reduction process.

As a final experiment, identical carbon cloth electrodes underwent a first ORR (discharge under oxygen) in LiTFSI and $LiNO_3$ solutions. At the end of these processes, cells were dismantled, the electrodes were thoroughly washed with pure solvent, and then underwent charging processes in fresh Li-O_2 cells loaded with the alternate solution. The voltage profiles thus obtained are presented in Figure 10. For ORR, typical and

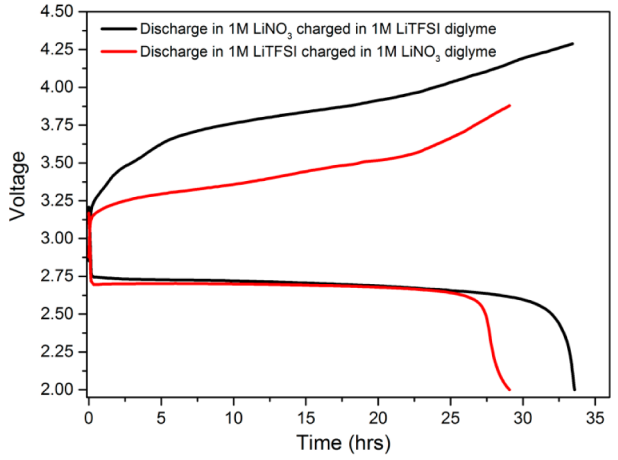

Figure 10. Voltage profiles of carbon paper electrodes (red curve) cell discharge in diglyme 1 M LiTFSI and charged in diglyme 1 M $LiNO_3$ (black curve), and discharge in diglyme 1 M $LiNO_3$ and charged in diglyme 1 M LiTFSI.

expected voltage profiles were obtained in each solution, as discussed above. The OER voltage profiles thus obtained were also typical to the second electrolyte solution used, no matter in which solution the ORR was carried out. Hence, the unique catalytic effect of $LiNO_3$ solutions on OER upon charging is clearly emphasized by these measurements.

CONCLUSIONS

Using $LiNO_3$ in polyether solutions as the electrolyte for Li-O_2 cells dramatically improves both oxygen reduction (ORR, discharge) and evolution (OER, charge) reactions. On the basis of extensive previous work, we suggest that, during ORR, the NO_3^- anions stabilize the Li^+ cations, thus reducing their Lewis acidity. This reduction results from the strong association between nitrate anions and Li cations in the ethereal solutions. As a result, the lifetime of the radical anions (superoxide and peroxide moieties) formed by oxygen reduction is extended because their immediate interaction with the Li ions (which promote precipitation of Li_2O_2 as the final product) is retarded. Hence, oxygen reduction occurs in the first stage under no passivation conditions, and soluble products accumulate in the solution phase. This situation promotes a top-down mechanism for Li_2O_2 precipitation that enables accumulation of thick particles on the cathodes' surface and a relatively high specific capacity (per electrode weight and volume). This situation is advantageous for ORR compared to the regular bottom-up precipitation mechanism of Li_2O_2 in LiTFSI solutions. The latter blocks and shuts down the process when the uniform insulating product layer is thus formed and reaches a certain nanometric thickness.

DOI: 10.1021/acsami.5b04145
ACS Appl. Mater. Interfaces 2015, 7, 16590−16600

The NO_3^- anions are reduced on the Li anode to various products, some of which are insoluble, assisting the Li metal anode passivation in solution. Nitrate anion reduction by lithium obviously forms soluble nitrite (NO_2^-) moieties, which are oxidized to NO_2 around 3.6−3.8 V relatice to Li. Althoguh NO_3^- and NO_2^- do not interact with Li_2O_2 due to their anionic nature, NO_2 can easily oxidize Li_2O_2 once it forms at potentials below 4 V. This oxidation process is catalytic, as the NO_2^- formed by NO_2 reduction (in the course of Li_2O_2 oxidation) is immediately reoxidized. As a result, only a small amount of nitrite moiety is required to fully oxidize all of the Li_2O_2 during OER below 4 V by the redox activity of the NO_2/NO_2^- couple.

Despite the positive benefits of the use of $LiNO_3$ as an electrolyte in polyether solutions as described above, we cannot ignore that the polyether solutions are not really stable in Li-O_2 cells. In fact, a large assortment of polar aprotic solvents decompose in Li-O_2 cells by reacting with the highly reactive peroxide and superoxide species formed via oxygen reduction. There are also inevitable continuous irreversible side reactions on the Li metal anodes. Some of the side products, such as alkoxides and carbonates, derived from solvent decomposition can be oxidized at relatively low potentials in parallel to the OER. However, the inevitable side reactions also form products that cannot be oxidized, which precipitate and passivate the cathodes.

We close by noting that in practical battery systems, with a relatively low ratio between electrolyte solution volume and electrodes' surface, the effect of these inevitable side reactions is seriously detrimental. Before promoting Li-O_2 cells as a promising practical battery technology, a systematic study of all possible key components of the Li-O_2 systems (electrodes, solvents, electrolytes) is a mandatory preliminary step. We believe that such systematic and careful studies may be able to elucidate stable components that can enable the development of working, rechargeable Li-O_2 batteries.

EXPERIMENTAL SECTION

Materials. $LiNO_3$ (99.999%) purchased from Alfa Aesar and $LiN(SO_2CF3)_2$ (99.95%) purchased from Sigma-Aldrich were dried under high vacuum. Diglyme (99.5%) was purchased from Sigma-Aldrich and later dried under a molecular sieve. Monolithic carbon paper was used as cathodes (Marketech International, USA) after reductive treatment in Ar/H_2 95:5 for 10 h at 900 °C (400 m^2/gr). Glassy separators were purchased from Whatman, and polyethylene separators were purchased from Cellguard. Gold cathodes were prepared by thin layer sputtering (25 °C, 100 W, and 5×10^{-3} mbar; Bestec) of gold (20 nm) on aluminum foil (99.9%; Strem Chemicals).

Products Analysis. An Inspect FEI microscope was employed for the high resolution scanning electron microscopy (HR-SEM) studies of pristine and cycled electrodes. The presence of lithium oxides on carbon and gold electrodes was analyzed using a Bruker D8 Advance X-ray Diffractometer (2θ = 30−70°) working with Cu Kα radiation (λ = 0.15418 nm). X-ray photoelectron spectroscopy (XPS) analysis of cycled electrodes was carried out using a Kratos Axis HS spectrometer (England) equipped with an Al Kα X-ray radiation source (photon energy = 1486.6 eV). A homemade transfer system, equipped with a gate valve and a magnetic manipulator, was used for the transfer of the highly sensitive samples from the highly pure argon atmosphere of the glovebox to the XPS system

EQCM Measurements. Electrochemical quartz crystal microbalance (EQCM) measurements were carried out with a GAMRY (Warminster, PA, USA) EQCM system. The working electrodes for these studies were gold discs deposited on 5 MHz AT-cut quartz crystals (1.38 cm^2) (SRS, Sunnyvale, CA, USA). A 3 mL electrochemical cell made of glass containing lithium counter and reference electrodes was used for EQCM measurements. Before measurements, the electrolyte solutions were bubbled with high-purity oxygen for 30 min.

Li-Oxygen Cell Operation. Cells were prepared from monolithic carbon paper cathodes in 1 M diglyme solutions of LiTFSI or $LiNO_3$ with a lithium metal anode. A glassy separator in between two polyethylene separators were incorporated into each cell. The cell contained a Teflon body squeezed between two stainless steel plates and two valves for insertion of pure oxygen. For impedance measurements, we added lithium metal R.E. between the two separators. Each cell was flushed with pure oxygen for 1 min and then held at 1 atm of oxygen for the rest of the experiment.

AUTHOR INFORMATION

Corresponding Author

*E-mail: Doron.Aurbach@biu.ac.il.

Author Contributions

⊥D.S and D.H contributed equally to this work.

Notes

The authors declare no competing financial interest.

ACKNOWLEDGMENTS

Partial support for this work was obtained from the ISF, Israel Science Foundation, in the framework of the INREP project and the Ministry of Science and Technology, Israel. A.A.F. thanks the Israel Science Foundation (Grant No. 1469/13) as well as the Ethel and David Resnick Chair in Active Oxygen Chemistry for their kind and generous support.

REFERENCES

(1) Thackeray, M. M.; Wolverton, C.; Isaacs, E. D. Electrical Energy Storage for Transportation—approaching the Limits Of, and Going Beyond, Lithium-Ion Batteries. *Energy Environ. Sci.* **2012**, *5* (7), 7854−7863.

(2) Armand, M.; Tarascon, J. Building Better Batteries. *Nature* **2008**, *451*, 652−657.

(3) Bruce, P. G.; Freunberger, S. A.; Hardwick, L. J.; Tarascon, J.-M. Li-O_2 and Li-S Batteries with High Energy Storage. *Nat. Mater.* **2011**, *11* (1), 19−29.

(4) Ottakam Thotiyl, M. M.; Freunberger, S. a.; Peng, Z.; Bruce, P. G. The Carbon Electrode in Nonaqueous Li-O_2 Cells. *J. Am. Chem. Soc.* **2013**, *135* (1), 494−500.

(5) McCloskey, B. D.; Bethune, D. S.; Shelby, R. M.; Girishkumar, G.; Luntz, A. C. Solvents' Critical Role in Nonaqueous Lithium−Oxygen Battery Electrochemistry. *J. Phys. Chem. Lett.* **2011**, *2* (10), 1161−1166.

(6) Bryantsev, V. S.; Blanco, M. Computational Study of the Mechanisms of Superoxide-Induced Decomposition of Organic Carbonate-Based Electrolytes. *J. Phys. Chem. Lett.* **2011**, *2* (5), 379−383.

(7) Assary, R. S.; Lau, K. C.; Amine, K.; Sun, Y.; Curtiss, L. A. Interactions of Dimethoxy Ethane with Li_2O_2 Clusters and Likely Decomposition Mechanisms for Li-O_2 Batteries. *J. Phys. Chem. C* **2013**, *117* (16), 8041−8049.

(8) Freunberger, S. a; Chen, Y.; Peng, Z.; Griffin, J. M.; Hardwick, L. J.; Bardé, F.; Novák, P.; Bruce, P. G. Reactions in the Rechargeable Lithium-O_2 Battery with Alkyl Carbonate Electrolytes. *J. Am. Chem. Soc.* **2011**, *133* (20), 8040−8047.

(9) Bryantsev, V. S.; Giordani, V.; Walker, W.; Blanco, M.; Zecevic, S.; Sasaki, K.; Uddin, J.; Addison, D.; Chase, G. V. Predicting Solvent Stability in Aprotic Electrolyte Li-Air Batteries: Nucleophilic Substitution by the Superoxide Anion Radical ($O_2(\bullet-)$). *J. Phys. Chem. A* **2011**, *115* (44), 12399−12409.

(10) Sharon, D.; Etacheri, V.; Garsuch, A.; Afri, M.; Frimer, A. A.; Aurbach, D. On the Challenge of Electrolyte Solutions for Li-Air Batteries: Monitoring Oxygen Reduction and Related Reactions in Polyether Solutions by Spectroscopy and EQCM. *J. Phys. Chem. Lett.* **2013**, *4* (1), 127−131.

DOI: 10.1021/acsami.5b04145
ACS Appl. Mater. Interfaces 2015, 7, 16590−16600

(11) Ryan, K. R.; Trahey, L.; Ingram, B. J.; Burrell, A. K. Limited Stability of Ether-Based Solvents in Lithium−Oxygen Batteries. *J. Phys. Chem. C* **2012**, *116* (37), 19724−19728.
(12) Khetan, A.; Pitsch, H.; Viswanathan, V. Solvent Degradation in Nonaqueous Li-O_2 Batteries: Oxidative Stability versus H-Abstraction. *J. Phys. Chem. Lett.* **2014**, *5*, 2419−2424.
(13) Viswanathan, V.; Thygesen, K. S.; Hummelshj, J. S.; Nrskov, J. K.; Girishkumar, G.; McCloskey, B. D.; Luntz, a C. Electrical Conductivity in Li_2O_2 and Its Role in Determining Capacity Limitations in Non-Aqueous Li-O_2 Batteries. *J. Chem. Phys.* **2011**, *135* (21), 214704−214714.
(14) McCloskey, B. D.; Speidel, A.; Scheffler, R.; Miller, D. C.; Viswanathan, V.; Hummelshøj, J. S.; Nørskov, J. K.; Luntz, A. C. Twin Problems of Interfacial Carbonate Formation in Nonaqueous Li-O_2 Batteries. *J. Phys. Chem. Lett.* **2012**, *3* (8), 997−1001.
(15) Gutmann, V. Solvent Effects on the Reactivities of Organometallic Compounds. *Coord. Chem. Rev.* **1976**, *18* (2), 225−255.
(16) Trahan, M. J.; Mukerjee, S.; Plichta, E. J.; Hendrickson, M. A.; Abraham, K. M. Studies of Li-Air Cells Utilizing Dimethyl Sulfoxide-Based Electrolyte. *J. Electrochem. Soc.* **2012**, *160* (2), A259−A267.
(17) Schroeder, M. A.; Kumar, N.; Pearse, A. J.; Liu, C.; Lee, S. B.; Rubloff, G. W.; Leung, K.; Noked, M. The DMSO-Li_2O_2 Interface in the Rechargeable Li-O_2 Battery Cathode: Theoretical and Experimental Perspectives on Stability. *ACS Appl. Mater. Interfaces* **2015**, *7*, 11402−11411.
(18) Walker, W.; Giordani, V.; Uddin, J.; Bryantsev, V. S.; Chase, G. V.; Addison, D. A Rechargeable Li-O_2 Battery Using a Lithium nitrate/N,N-Dimethylacetamide Electrolyte. *J. Am. Chem. Soc.* **2013**, *135* (6), 2076−2079.
(19) Johnson, L.; Li, C.; Liu, Z.; Chen, Y.; Freunberger, S. A.; Tarascon, J.-M.; Ashok, P. C.; Praveen, B. B.; Dholakia, K.; Bruce, P. G. The Role of LiO_2 Solubility in O_2 Reduction in Aprotic Solvents and Its Consequences for Li-O_2 Batteries. *Nat. Chem.* **2014**, *6* (12), 1091−1099.
(20) Meini, S.; Piana, M.; Tsiouvaras, N.; Garsuch, A.; Gasteiger, H. a. The Effect of Water on the Discharge Capacity of a Non-Catalyzed Carbon Cathode for Li-O_2 Batteries. *Electrochem. Solid-State Lett.* **2012**, *15* (4), A45−A48.
(21) Sharon, D.; Afri, M.; Noked, M.; Garsuch, A.; Frimer, A. A.; Aurbach, D. Oxidation of Dimethyl Sulfoxide Solutions by Electrochemical Reduction of Oxygen. *J. Phys. Chem. Lett.* **2013**, *4* (18), 3115−3119.
(22) Aetukuri, N. B.; McCloskey, B. D.; García, J. M.; Krupp, L. E.; Viswanathan, V.; Luntz, A. C. Solvating Additives Drive Solution-Mediated Electrochemistry and Enhance Toroid Growth in Non-Aqueous Li-O_2 Batteries. *Nat. Chem.* **2014**, *7*, 50−56.
(23) Lim, H.; Song, H.; Kim, J.; Gwon, H.; Bae, Y.; Park, K.; Hong, J.; Kim, H.; Kim, T.; Kim, Y. H.; Kang, K. Superior Rechargeability and Efficiency of Lithium-Oxygen Batteries: Hierarchical Air Electrode Architecture Combined with a Soluble Catalyst. *Angew. Chem., Int. Ed.* **2014**, *53* (15), 3926−3931.
(24) Bergner, B. J.; Schürmann, A.; Peppler, K.; Garsuch, A.; Janek, J. TEMPO: A Mobile Catalyst for Rechargeable Li-O_2 Batteries. *J. Am. Chem. Soc.* **2014**, *136*, 15054−15064.
(25) Chen, Y.; Freunberger, S. A.; Peng, Z.; Fontaine, O.; Bruce, P. G. Charging a Li-O_2 Battery Using a Redox Mediator. *Nat. Chem.* **2013**, *5* (6), 489−494.
(26) Kwak, W.-J.; Hirshberg, D.; Sharon, D.; Shin, H.-J.; Afri, M.; Park, J.-B.; Garsuch, A.; Chesneau, F. F.; Frimer, A. a.; Aurbach, D.; Sun, Y. Y. Understanding the Behavior of Li-Oxygen Cells Containing LiI. *J. Mater. Chem. A* **2015**, *3*, 8855−8864.
(27) Aurbach, D.; Pollak, E.; Elazari, R.; Salitra, G.; Kelley, C. S.; Affinito, J. On the Surface Chemical Aspects of Very High Energy Density, Rechargeable Li−Sulfur Batteries. *J. Electrochem. Soc.* **2009**, *156* (8), A694−A702.
(28) Zhang, S. S. Role of $LiNO_3$ in Rechargeable Lithium/sulfur Battery. *Electrochim. Acta* **2012**, *70*, 344−348.
(29) Liang, X.; Wen, Z.; Liu, Y.; Wu, M.; Jin, J.; Zhang, H.; Wu, X. Improved Cycling Performances of Lithium Sulfur Batteries with $LiNO_3$-Modified Electrolyte. *J. Power Sources* **2011**, *196* (22), 9839−9843.
(30) Giordani, V.; Walker, W.; Bryantsev, V. S.; Uddin, J.; Chase, G. V.; Addison, D. Synergistic Effect of Oxygen and $LiNO_3$ on the Interfacial Stability of Lithium Metal in a Li/O_2 Battery. *J. Electrochem. Soc.* **2013**, *160* (9), A1544−A1550.
(31) Chen, Y.; Freunberger, S. A.; Peng, Z.; Bardé, F.; Bruce, P. G. Li-O_2 Battery with a Dimethylformamide Electrolyte. *J. Am. Chem. Soc.* **2012**, *134* (18), 7952−7957.
(32) Sharon, D.; Hirsberg, D.; Afri, M.; Garsuch, A.; Frimer, A. A.; Aurbach, D. Reactivity of Amide Based Solutions in Lithium−Oxygen Cells. *J. Phys. Chem. C* **2014**, *118* (28), 15207−15213.
(33) Kang, S. J.; Mori, T.; Narizuka, S.; Wilcke, W.; Kim, H.-C. Deactivation of Carbon Electrode for Elimination of Carbon Dioxide Evolution from Rechargeable Lithium-Oxygen Cells. *Nat. Commun.* **2014**, *5*, 3937−3943.
(34) Sun, B.; Huang, X.; Chen, S.; Zhang, J.; Wang, G. An Optimized $LiNO_3$/DMSO Electrolyte for High-Performance Rechargeable Li-O_2 Batteries. *RSC Adv.* **2014**, *4* (22), 11115−11120.
(35) Gunasekara, I.; Mukerjee, S.; Plichta, E. J.; Hendrickson, M. a.; Abraham, K. M. A Study of the Influence of Lithium Salt Anions on Oxygen Reduction Reactions in Li-Air Batteries. *J. Electrochem. Soc.* **2015**, *162* (6), A1055−A1066.
(36) Henderson, W. A. Glyme-Lithium Salt Phase Behavior. *J. Phys. Chem. B* **2006**, *110*, 13177−13183.
(37) Henderson, W. A. Crystallization Kinetics of Glyme−LiX and PEO−LiX Polymer Electrolytes. *Macromolecules* **2007**, *40*, 4963−4971.
(38) Ueno, K.; Yoshida, K.; Tsuchiya, M.; Tachikawa, N.; Dokko, K.; Watanabe, M. Glyme-Lithium Salt Equimolar Molten Mixtures: Concentrated Solutions or Solvate Ionic Liquids? *J. Phys. Chem. B* **2012**, *116*, 11323−11331.
(39) Seo, D. M.; Borodin, O.; Han, S.-D.; Ly, Q.; Boyle, P. D.; Henderson, W. A. Electrolyte Solvation and Ionic Association. *J. Electrochem. Soc.* **2012**, *159* (5), A553−A565.
(40) Sharon, D.; Hirshberg, D.; Afri, M.; Garsuch, A.; Frimer, A. A.; Aurbach, D. Lithium-Oxygen Electrochemistry in Non-Aqueous Solutions. *Isr. J. Chem.* **2015**, *55* (5), 508−520.
(41) Ganapathy, S.; Adams, B. D.; Stenou, G.; Anastasaki, M. S.; Goubitz, K.; Miao, X.; Nazar, L. F.; Wagemaker, M. Nature of Li_2O_2 Oxidation in a Li-O_2 Battery Revealed by Operando X-Ray Diffraction. *J. Am. Chem. Soc.* **2014**, *136*, 16335−16344.
(42) Rosenman, A.; Elazari, R.; Salitra, G.; Markevich, E.; Aurbach, D.; Garsuch, a. The Effect of Interactions and Reduction Products of $LiNO_3$, the Anti-Shuttle Agent, in Li-S Battery Systems. *J. Electrochem. Soc.* **2015**, *162* (3), A470−A473.
(43) Strickler, S. J.; Kasha, M. Solvent Effects on the Electronic Absorption Spectrum of Nitrite Ion. *J. Am. Chem. Soc.* **1963**, *85* (11), 2899−2901.
(44) Uddin, J.; Bryantsev, V. S.; Giordani, V.; Walker, W.; Chase, G. V.; Addison, D. Lithium Nitrate As Regenerable SEI Stabilizing Agent for Rechargeable Li-O_2 Batteries. *J. Phys. Chem. Lett.* **2013**, *4* (21), 3760−3765.
(45) Meini, S.; Tsiouvaras, N.; Schwenke, K. U.; Piana, M.; Beyer, H.; Lange, L.; Gasteiger, H. A. Rechargeability of Li-Air Cathodes Pre-Filled with Discharge Products Using an Ether-Based Electrolyte Solution: Implications for Cycle-Life of Li-Air Cells. *Phys. Chem. Chem. Phys.* **2013**, *15* (27), 11478−11493.
(46) Freunberger, S. A.; Chen, Y.; Drewett, N. E.; Hardwick, L. J.; Bardé, F.; Bruce, P. G. The Lithium-Oxygen Battery with Ether-Based Electrolytes. *Angew. Chem., Int. Ed.* **2011**, *50* (37), 8609−8613.
(47) Leskes, M.; Moore, A. J.; Goward, G. R.; Grey, C. P. Monitoring the Electrochemical Processes in the Lithium-Air Battery by Solid State NMR Spectroscopy. *J. Phys. Chem. C* **2013**, *117* (51), 26929−26939.
(48) Meini, S.; Solchenbach, S.; Piana, M.; Gasteiger, H. A. The Role of Electrolyte Solvent Stability and Electrolyte Impurities in the Electrooxidation of Li_2O_2 in Li-O_2 Batteries. *J. Electrochem. Soc.* **2014**, *161* (9), A1306−A1314.

DOI: 10.1021/acsami.5b04145
ACS Appl. Mater. Interfaces 2015, 7, 16590−16600

(49) McCloskey, B. D.; Bethune, D. S.; Shelby, R. M.; Mori, T.; Scheffler, R.; Speidel, A.; Sherwood, M.; Luntz, a C. Limitations in Rechargeability of Li-O2Batteries and Possible Origins. *J. Phys. Chem. Lett.* **2012**, *3*, 3043−3047.
(50) Yeager, H. L.; Reid, H. Spectroscopic Studies of Ionic Association in Propylene Carbonate. *J. Phys. Chem.* **1976**, *80* (8), 850−853.
(51) Schwenke, K. U.; Metzger, M.; Restle, T.; Piana, M.; Gasteiger, H. A. The Influence of Water and Protons on Li_2O_2 Crystal Growth in Aprotic Li-O_2 Cells. *J. Electrochem. Soc.* **2015**, *162* (4), A573−A584.
(52) Andersen, C. P.; Hu, H.; Qiu, G.; Kalra, V.; Sun, Y. Pore-Scale Transport Resolved Model Incorporating Cathode Microstructure and Peroxide Growth in Lithium-Air Batteries. *J. Electrochem. Soc.* **2015**, *162* (7), A1135−A1145.

DOI: 10.1021/acsami.5b04145
ACS Appl. Mater. Interfaces 2015, 7, 16590−16600